Electronic supporting information

Superassembled MXene-Carboxymethyl Chitosan Nanochannels for High-Sensitive Recognition and Detection of Copper Ions

Xiaomeng Hu,[a] Shan Zhou,[b] Xin Zhang,[a] Hui Zeng,[a] Yaxin Guo,[a] Yeqing Xu,[a] Qirui Liang,[a,c] Jinqiang Wang,[d] Lei Jiang,[e] and Biao Kong[a,f,*]

[a]Department of Chemistry, Shanghai Key Lab of Molecular Catalysis and Innovative Materials and Collaborative Innovation Center of Chemistry for Energy Materials, Fudan University, Shanghai 200438, P. R. China.

[b]College of Materials Science and Engineering, Institute of Biomedical Materials and Engineering, Qingdao University, Qingdao 266071, P. R. China

[c]Qingdao Innovation and Development Center, Harbin Engineering University, Qingdao 266400, P. R. China

[d]Key Laboratory of Advanced Drug Delivery Systems of Zhejiang Province, College of Pharmaceutical Sciences, Zhejiang University, Hangzhou 310058, P. R. China

[e]CAS Key Laboratory of Bio-Inspired Materials and Interfacial Science, Technical Institute of Physics and Chemistry, Chinese Academy of Science, Beijing 100190, P. R. China

[f]Yiwu Research Institute of Fudan University, Yiwu, Zhejiang 322000, P. R. China

*Corresponding author: Biao Kong (B.K.)

Email address: bkong@fudan.edu.cn

Table of contents

1. Characterization of MXene/CMC and MXene nanosheets

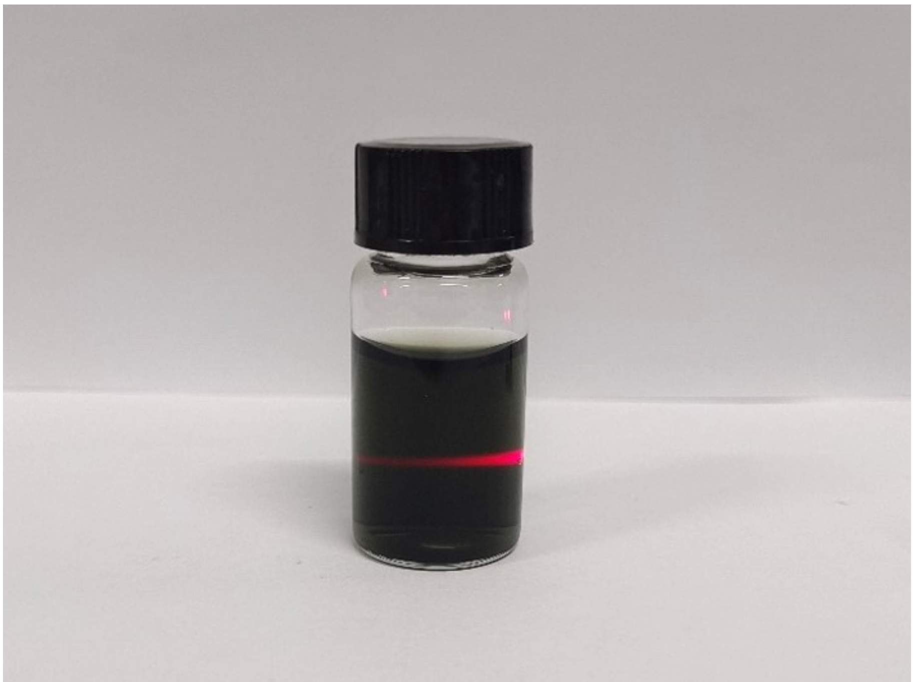

Fig. S1 The Tyndall scattering effect[1] of the as-prepared MXene/CMC suspension, indicating the good dispersion in water.

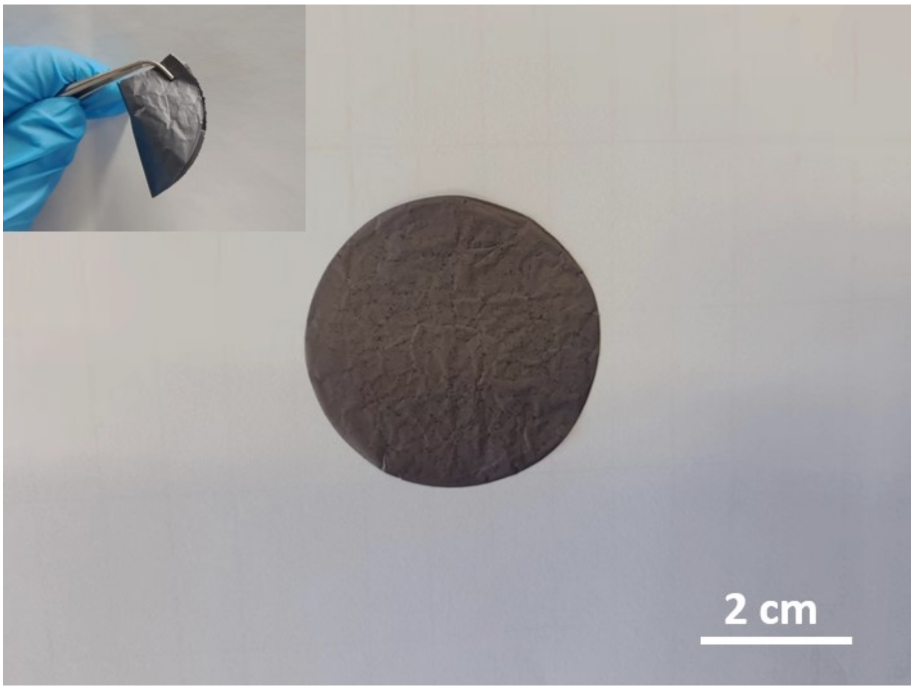

Fig. S2 Photographs of the freestanding and flexible MXene/CMC membrane.

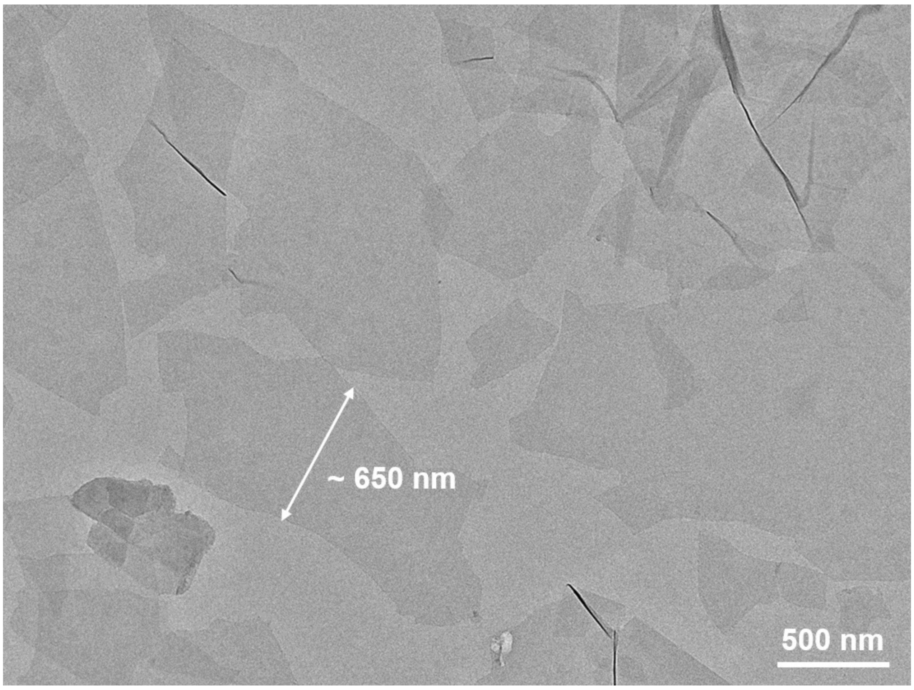

Fig. S3 TEM image of thin MXene nanosheets.

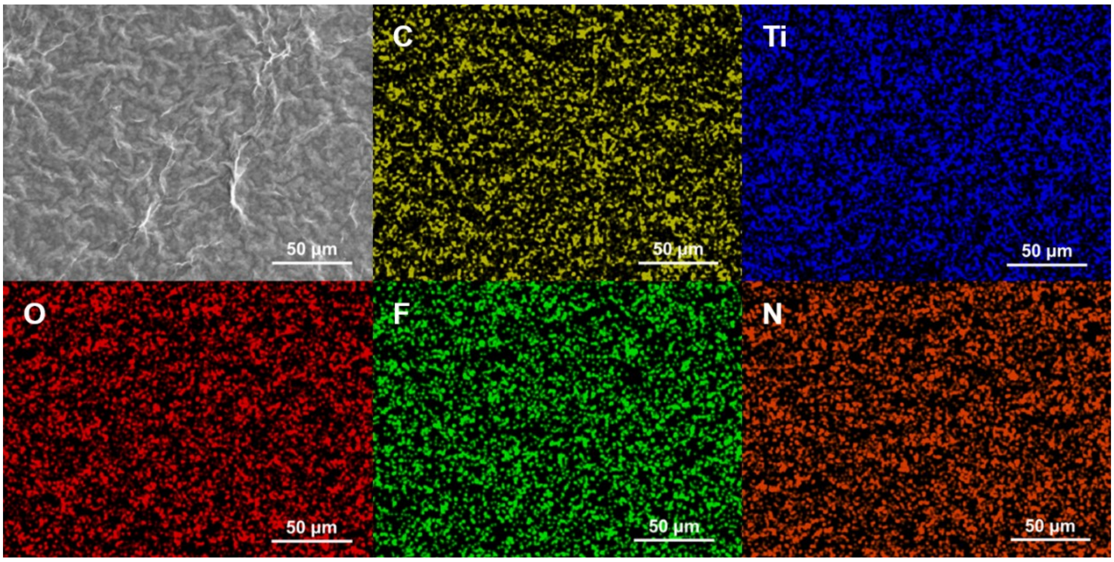

Fig. S4 EDX mapping of the C, Ti, O, F and N distribution on the surface of the MXene/CMC membrane.

2. Ion transport performance of MXene/CMC

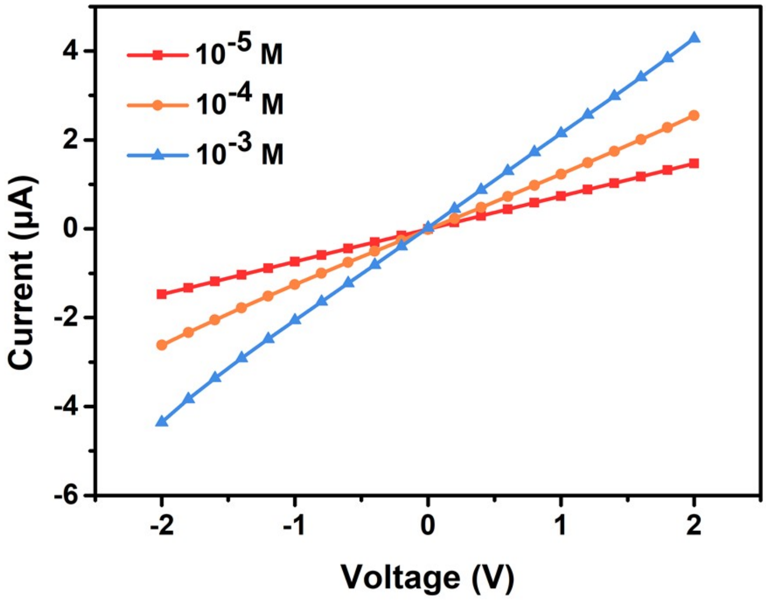

Fig. S5 Current–voltage (I–V) curves of MXene/CMC membrane (CMC weight content of 20%) recorded in neutral KCl electrolyte with different concentrations.

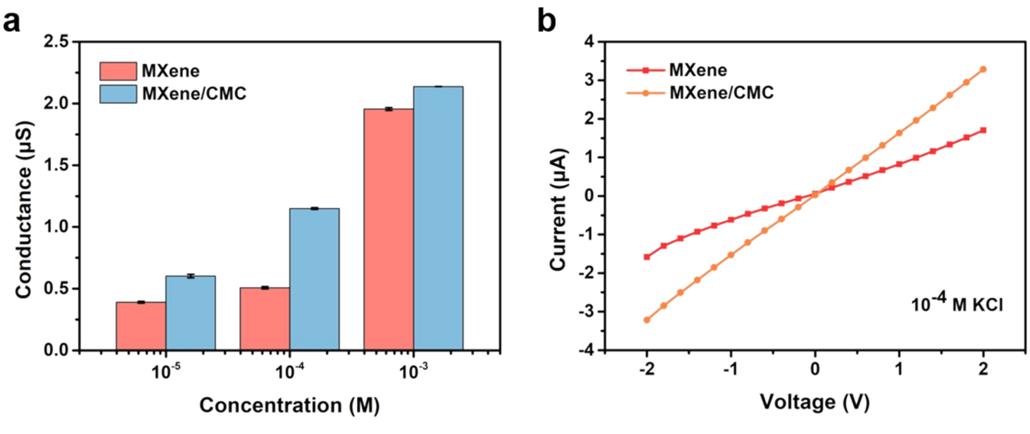

Fig. S6 The variation of (a) conductance and (b) current–voltage (I–V) curves of different membranes.

3. Characterization of MXene/CMC with divalent metal ions

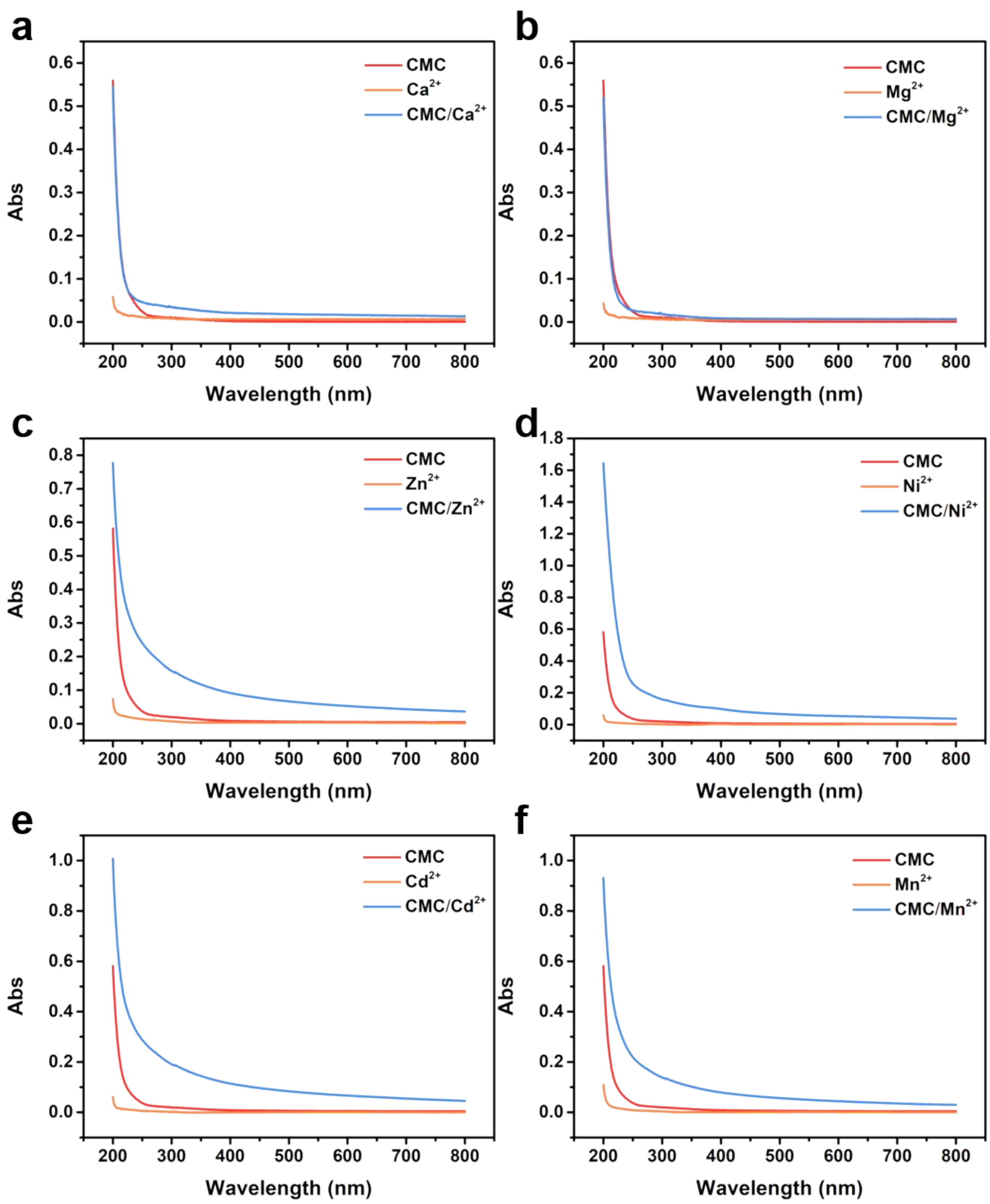

Fig. S7 UV−Vis absorption spectra of CMC with different divalent metal ions (1 mM). (a) Ca^{2+}, (b) Mg^{2+}, (c) Zn^{2+}, (d) Ni^{2+}, (e) Cd^{2+} and (f) Mn^{2+}.

4. XPS spectrum of O 1s and N 1s of membranes

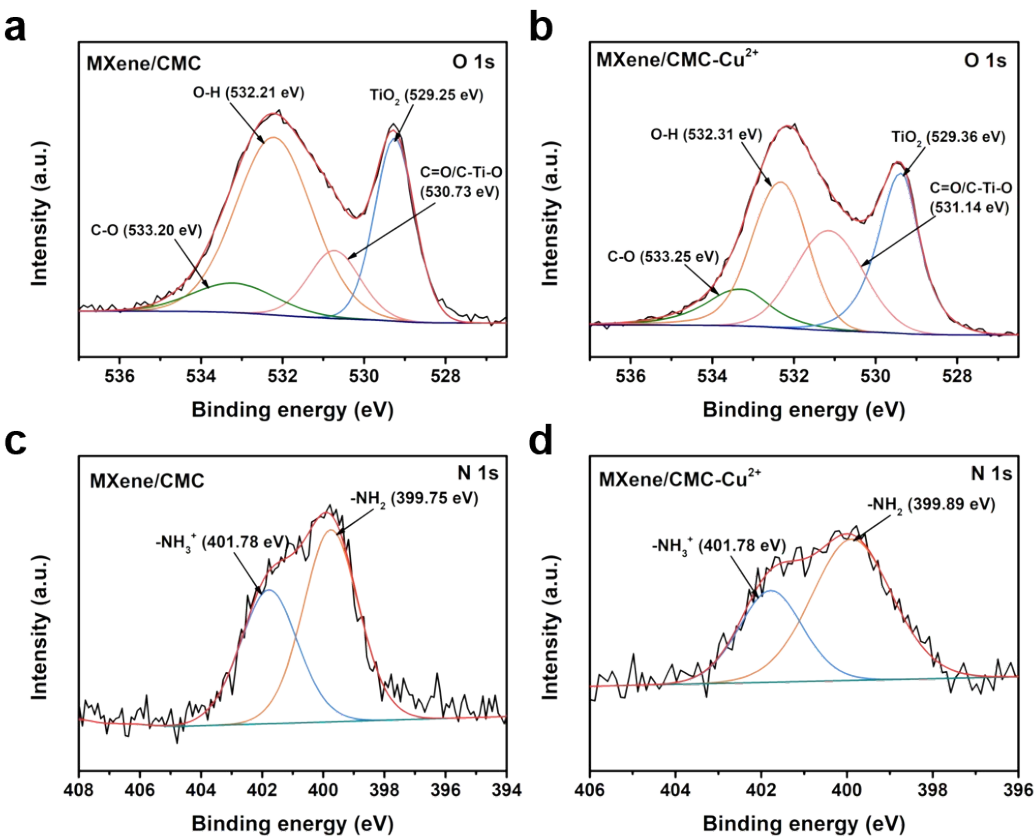

Fig. S8 XPS spectrum of O 1s of (a) MXene/CMC and (b) MXene/CMC-Cu^{2+}, respectively. XPS spectrum of N 1s of (c) MXene/CMC and (d) MXene/CMC-Cu^{2+}, respectively.

5. Influence of CMC content on Cu^{2+} detection

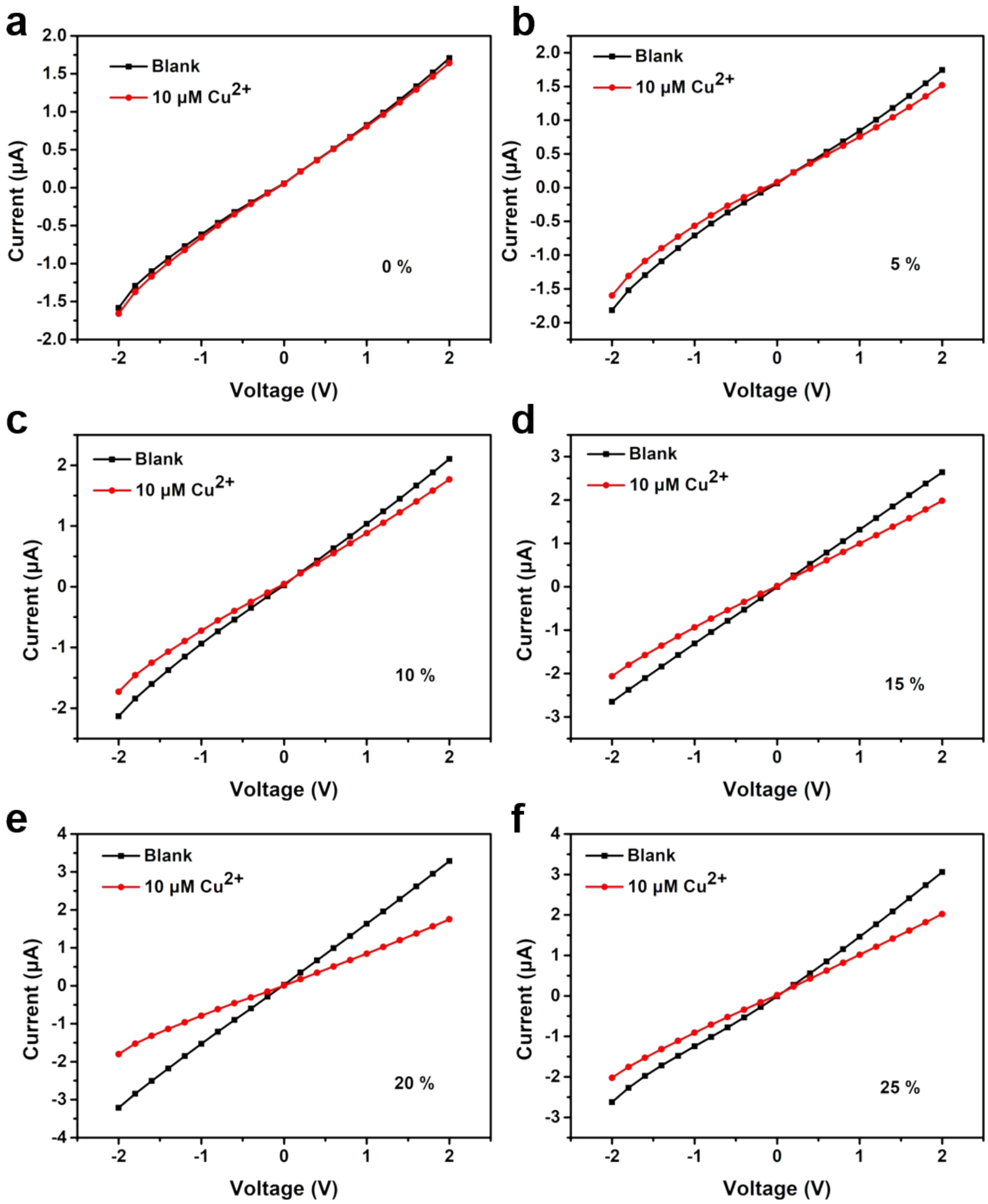

Fig. S9 Influence of the CMC content of MXene/CMC membrane on Cu^{2+} detection. (a) 0%, (b) 5%, (c) 10%, (d) 15%, (e) 20%, and (f) 25%.

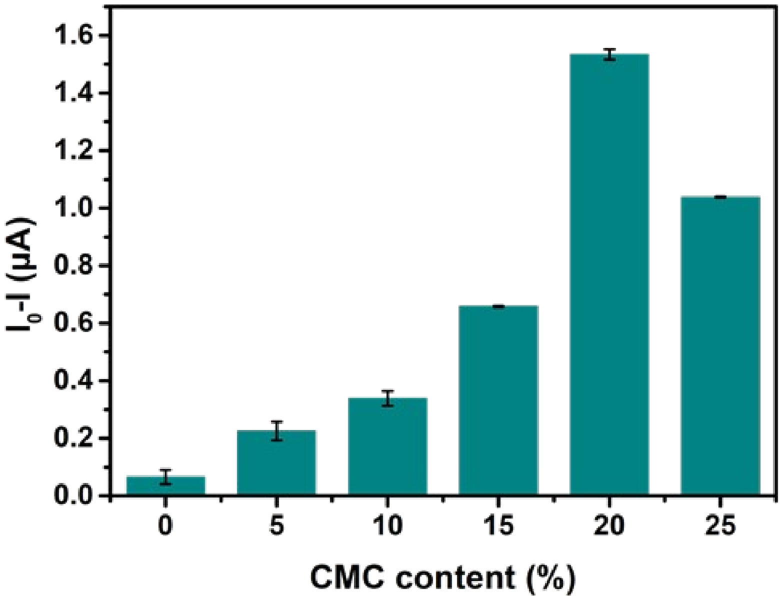

Fig. S10 Influence of CMC contents on the current change of MXene/CMC with the absence and the presence of 10 μM $CuCl_2$.

6. I−V of MXene/CMC under different Cu^{2+} concentrations

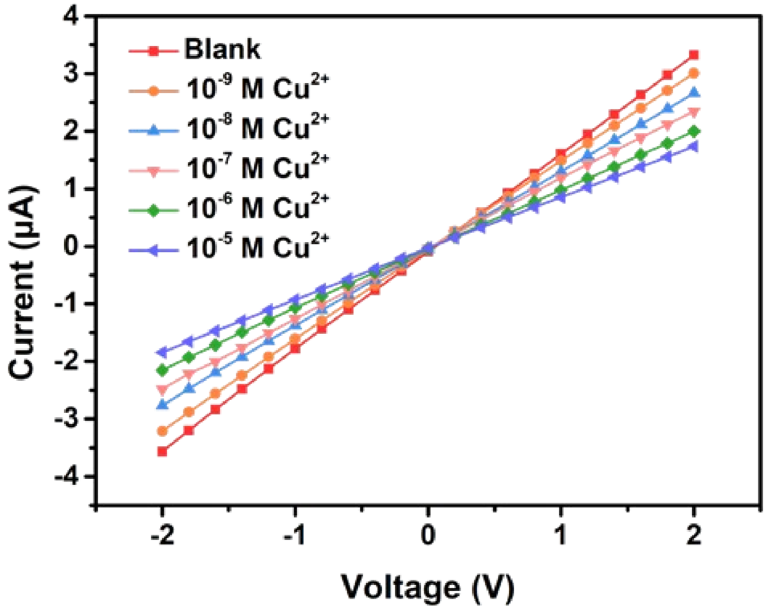

Fig. S11 I−V curves of MXene/CMC under different Cu^{2+} concentrations.

7. Zeta potential and water contact angles of nanochannels

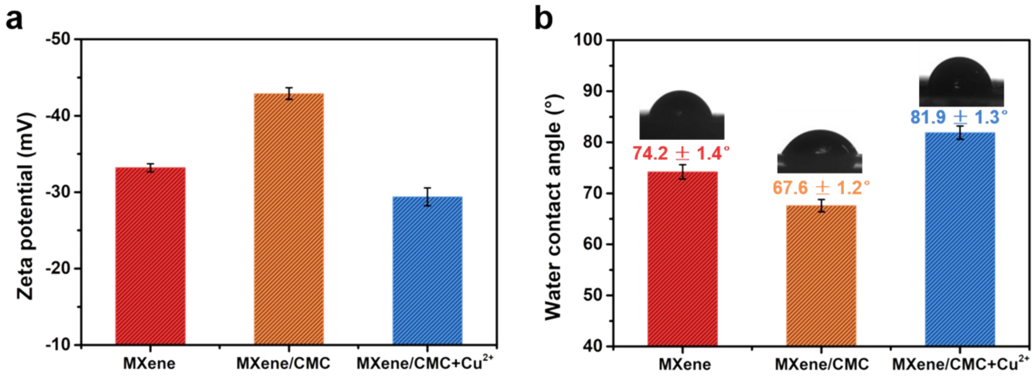

Fig. S12 (a) Zeta potential of MXene, MXene/CMC and MXene/CMC with Cu^{2+}. (b) Water contact angles of different nanochannels.

8. Detection of Cu^{2+} in real samples

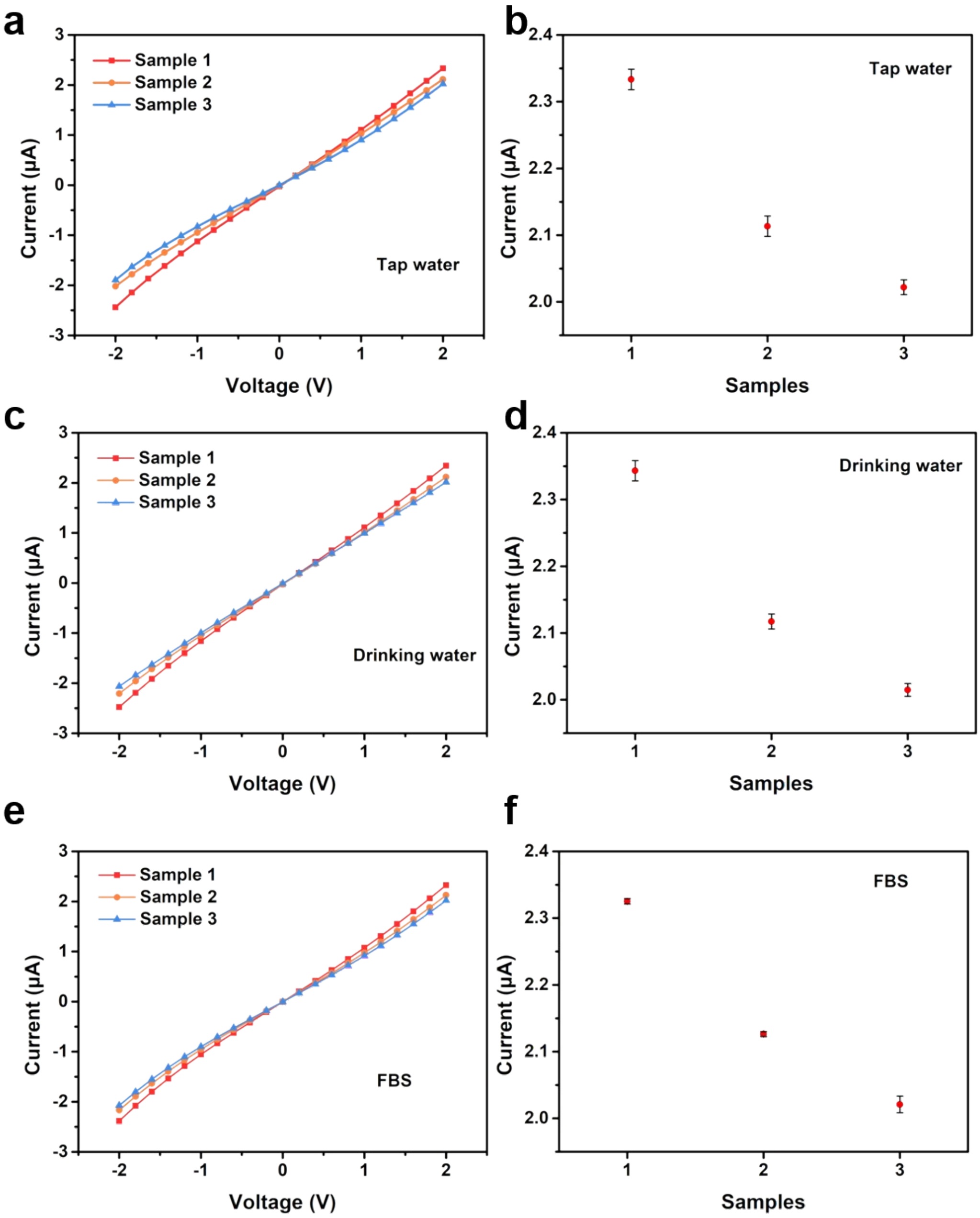

Fig. S13 Detection of Cu^{2+} in real samples. I−V profiles of different concentrations of Cu^{2+} in tap water (a), drinking water (c) and FBS (e) samples. Sample 1: 10 μM Cu^{2+} added, sample 2: 50 μM Cu^{2+} added and sample 3: 100 μM Cu^{2+} added. (b, d and f)Ionic current at +2 V versus different samples.

9. The dosage of different MXene/CMC composite membrane

Table S1. The dosage of different MXene/CMC composite membrane.

Items	0%	5%	10%	15%	20%	25%
MXene (V/mL)	10	10	10	10	10	10
CMC (V/mL)	0	0.5	1	1.5	2	2.5

10.Comparison of some methods reported for Cu^{2+} detection

Table S2. The sensing performance of different methods reported for Cu^{2+} detection

Materials	Methods	Linear range	Detection limit	Ref.
$Ti_3C_2T_x$@CB	DPV	0.01 - 15 μM	4.6 nM	2
GA-UiO-66-NH_2	DPSV	0.1 - 3.5 μM	7 nM	3
ZIF-67/EG	SWASV	0.5 - 3 μM	2.23 nM	4
PLA/GR	CV	0.08 - 1.6 mM	3.52 μM	5
Ni/NiO/ZnO-6/CS	DPV	0 - 6 μM	0.81 nM	6
N-Ti_3C_2 QDs	Fluorescence	50 nM - 1 mM	3 nM	7
PEIFPLP NP	Fluorescence	2.4 - 19 μM	17 nM	8
CdSe@ZIF-8/PAA	Nanochannels	0.01 pM - 1 μM	4 fM	9
MXene/CMC	Nanochannels	1 nM - 10 μM	0.095 nM	This work

11.Results of the detection of Cu^{2+} in tap water, drinking water, and FBS samples

Table S3. Results of the detection of Cu^{2+} in tap water, drinking water, and FBS samples

Samples	Added Cu^{2+}(μM)	Found Cu^{2+}(μM)	Recovery (%)	RSD (%)
Tap water	10	10.6	106	4.09
	50	51.2	102	4.07
	100	99	99	1.67
Drinking water	10	9.85	98.5	3.98
	50	49.8	99.7	3.57
	100	104	104	3.42
FBS	10	11.2	112	4.26
	50	46.7	93.4	4.56
	100	99.4	99.4	2.24

12.Supporting references

1. Z. Zhang, S. Yang, P. Zhang, J. Zhang, G. Chen and X. Feng, *Nat. Commun.*, 2019, **10**, 2920.

2. Y. Xia, Y. Ma, Y. Wu, Y. Yi, H. Lin and G. Zhu, *Microchim. Acta*, 2021, **188**, 377.

3. M. Lu, Y. Deng, Y. Luo, J. Lv, T. Li, J. Xu, S.-W. Chen and J. Wang, *Anal. Chem.*, 2019, **91**, 888-895.

4. L. Ma, X. Zhang, M. Ikram, M. Ullah, H. Wu and K. Shi, *Chem. Eng. J.*, 2020, **395**, 125216.

5. G. Chakraborty, V. Katiyar and G. Pugazhenthi, *Compos. Sci. Technol.*, 2021, **213**, 108877.

6. J. Yu, X. Zhang, M. Zhao, Y. Ding, Z. Li, Y. Ma, H. Li and H. Cui, *Anal. Chim. Acta*, 2021, **1143**, 45-52.

7. X. Zhou, J. Zhang, D. Huang, Y. Yi, K. Wu and G. Zhu, *Spectrochim. Acta. A*, 2023, **293**, 122484.

8. A. K. Saini and S. K. Sahoo, *ACS Appl. Nano Mater.*, 2023, **6**, 3277-3284.

9. H. Gao, R. Sun, L. He, Z.-J. Qian, C. Zhou, P. Hong, S. Sun, R. Mo and C. Li, *ACS Appl. Mater. Interfaces*, 2020, **12**, 4849-4858.